TECHNICAL TRANSACTIONS | **CZASOPISMO TECHNICZNE**
ELECTRICAL ENGINEERING | ELEKTROTECHNIKA
3-E/2016

DOI: 10.4467/2353737XCT.16.265.6064

DARIUSZ BORKOWSKI*

VOLTAGE AND FREQUENCY CONTROL OF A STAND-ALONE INDUCTION GENERATOR USING SVPWM CONVERTER IN A SMALL RESERVOIR HYDROPOWER PLANT

STEROWANIE CZĘSTOTLIWOŚCI I NAPIĘCIA AUTONOMICZNEGO GENERATORA INDUKCYJNEGO PRZEZ PRZEKSZTAŁTNIK SVPWM W ZBIORNIKOWEJ ELEKTROWNI WODNEJ

Abstract

Induction generators are widely used to generate electrical power in small hydraulic applications. The main disadvantage of stand-alone induction generators is the problem of regulating the voltage magnitude and voltage frequency under load variation. This paper investigates a three-phase self-excited induction generator (SEIG) operating under varying load, utilizing the water energy in a small reservoir hydropower plant. The generator excitation is provided by a three-phase capacitor bank and an inverter with Space Vector Pulse Width Modulation (SVPWM). Furthermore, the inverter with a battery controls the active power flow between the generator and the load in order to provide a constant frequency of voltage. The proposed control scheme consists of two PI controllers. The first controls the voltage magnitude by regulating the inverter reactive power, while the second one adjusts the guide vanes of the turbine according to the DC voltage of the battery. The proposed control system has been tested under load step changes. The simulation results of the system, obtained using the Matlab/Simulink software, have demonstrated good control performance.

Keywords: self-excited induction generator, SVPWM inverter, small hydropower plant, control algorithm

Streszczenie

Generatory indukcyjne są szeroko stosowane do produkcji energii elektrycznej w elektrowniach wodnych małej mocy. Główną wadą samowzbudnych generatorów indukcyjnych są problemy z regulacją amplitudy i częstotliwości napięcia podczas zmian obciążenia. W artykule przedstawiono wyniki badań układu generacji autonomicznej z maszyną indukcyjną przetwarzającą energię mechaniczną turbiny w zbiornikowej małej elektrowni wodnej. Moc bierna niezbędna do wzbudzenia maszyny dostarczana jest zarówno przez baterię kondensatorów oraz falownik napięcia sterowany z zastosowaniem metody modulacji wektorowej (SVPWM). Ponadto, falownik wyposażony jest w bufor energii (baterię) przez co może sterować przepływem mocy czynnej, a w rezultacie sterować częstotliwością napięcia. Proponowany system sterowany jest za pomocą dwóch regulatorów PI. Pierwszy steruje wartością napięcia poprzez dostarczanie mocy biernej, podczas gdy drugi reguluje kierownicą turbiny wodnej na podstawie napięcia w obwodzie DC. Zaprezentowany system został przetestowany podczas skokowej zmiany obciążenia. Przedstawiono symulacje pochodzące z modelu stworzonego w aplikacji Matlab/Simulink, które prezentują właściwości systemu.

Słowa kluczowe: samowzbudny generator indukcyjny, falowniki SVPWM, mała elektrownia wodna, algorytmy sterowania

* Ph.D. Eng. Dariusz Borkowski, Institute of Electromechanical Energy Conversion, Faculty of Electrical and Computer Engineering, Cracow University of Technology.

1. Introduction

Squirrel-cage induction generators are widely used in various applications, for instance: hydropower, wind turbines, biomass sources, fuel engine driven generation systems etc., especially in small-scale systems. This is caused by their low price, simple construction, robustness, ease of maintenance, and no separate excitation source [1].

The on-grid operation is simple and does not require any special synchronization procedure like synchronous generators. The induction machine starts generating active power when the rotor speed is greater than the synchronous speed defined by the frequency of the grid voltage. However, there is the need of reactive power compensation, which is often provided by the capacitor bank.

Induction generators can also be used in off-grid applications for supplying isolated areas. The voltage may be built-up either by the residual flux or by pre-charged capacitors connected in parallel to the machine. The main disadvantage of the self-excited induction generator (SEIG) is poor regulation of the frequency and magnitude of the generator stator voltage [2]. The frequency is affected by the load level due to the machine slip, while the magnitude depends mainly on the value of excitation capacitor, magnetization characteristics as well as electrical load and its power factor.

Induction generators may be operated at a constant speed or variable speed. The variable speed operation is often used in the systems where speed regulation may provide higher energy conversion efficiency of the turbine under changeable conditions, for instance in wind systems. However, it requires using a full-scale AC/DC/AC converter consisting of two back-to-back PWM inverters, which increases the control complexity, costs and decreases the overall system efficiency. Moreover, the induction generator efficiency is significantly affected by the power and speed variations [3].

In the recent literature, many control methods providing voltage and frequency regulation of the constant speed SEIG are presented. The basic voltage controllers use Thyristor Switched Capacitors (TSC) to adjust the terminal voltage [4], while other solutions employ a power electronic converter, such as Static Var Compensator (SVC) that provides voltage regulation [5] with an assumption of the constant speed operation. The simple speed governor controls the input mechanical torque in order to keep a constant frequency [6]. This solution characterizes poor regulation capabilities under dynamic transients due to the large mechanical time constants. Other structures, called ungoverned-speed-based systems, also employ the PWM inverters, but do not control the speed. The voltage regulation is done by consuming all exceeding energy of the generated power (not consumed by the load) by the controlled resistance acting as an electronic load controller [7] or sending it to the grid by a single-phase line [8]. The surplus energy may also be utilized by a controlled load like the variable frequency induction motor drive (VFIMD) [9]. New methods use two separate modules, known as a distribution static compensator and VFIMD, which control the voltage and the frequency separately [10]. The stabilization of the stator voltage amplitude of an induction generator can also be achieved using the field-orientation control strategy for PWM voltage source inverter [11]. This method ensures voltage amplitude stabilization even at high dynamic load changes and changes of rotor speed of the generator; however it requires a large number of processing signals to estimate the rotor flux space vector.

Very promising solutions use the voltage source inverter (VSI) with the battery energy storage system (BESS) [12, 13]. The battery is used to control the active power and thus adjusts the voltage frequency. The significant load variations require providing a large-size energy buffer. Moreover, these solutions are appropriate for the energy source systems that are suitable to operate under narrow speed variations also called the "constant-frequency systems". It means that the almost-constant speed cannot affect the energy conversion efficiency under changeable conditions. Taking into account turbine performance, this solution is rather suitable for hydropower than for wind turbines.

In this paper, the VSI with the BESS is employed to control the magnitude and frequency of the load voltage in a small hydropower plant. In order to minimize the battery size, power governor (input torque governor), in the form of the guide vane regulator, is implemented. The active power provided by the converter is used only in the dynamic transients, while the power governor is adjusting. The system model containing a squirrel-cage induction generator, converter with batteries and variable load is prepared in the Matlab/Simulink software using the power system blockset (PSB) toolboxes.

2. Description of the energy conversion system

The configuration of the analyzed energy conversion system is presented in Fig. 1. The induction generator is driven by the water turbine via a gearbox. A hydro-set also contains guide vanes, which control the amount of water flowing through the turbine. The excitation is provided by the capacitor bank and the voltage controller (VC), which consists of the VSI, the battery and a reactor. The VC acts as the bidirectional source of active and reactive power and controls the voltage in magnitude and frequency that are perturbed by the variable three-phase load.

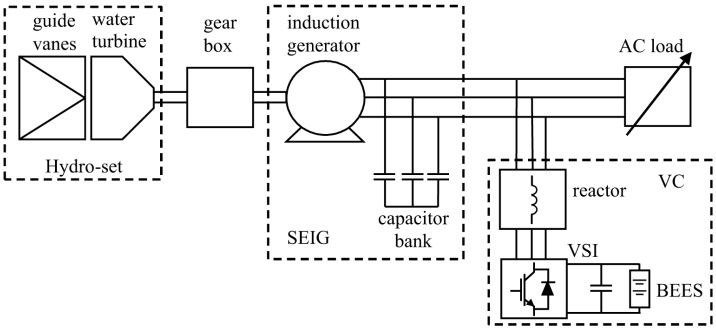

Fig. 1. Schematic diagram of the system configuration of the energy conversion system

3. Hydro-set model

In the paper, the reservoir hydropower plant is investigated, where stored water can be used when it is the most convenient. The main operation target is to utilize the water energy according to the energy demand of the load. This function is performed by guide

vanes, which control the turbine discharge. Assuming a constant water head, defined as the difference between the upper and the lower water level, the discharge corresponds to the water power potential. The output power of the water turbine is additionally affected by its efficiency (1).

$$P_t = 9.81 \cdot \rho_w \cdot Q \cdot H \cdot \eta \tag{1}$$

where:

- ρ_w – water density [kg/m^3],
- Q – water flow (turbine discharge) [m^3/s],
- H – difference of water level between the upstream level and the downstream level (water head) [m],
- η – turbine efficiency.

The turbine performance is usually visualized on the water discharge – speed plane, the so-called hill chart. It also presents the efficiency isolines that connect the operation points with the same efficiency. This chart is obtained from mathematical modelling or it is identified on the site after turbine installation. Using formula (1) and the hill chart, it is possible to approximate the relative torque of the turbine by a polynomial function of relative speed (2) with constants that are guide vane angle functions [14].

$$T_t^r = C_H \cdot \left(a(\alpha) \cdot n_t^{r2} + b(\alpha) \cdot n_t^r + c(\alpha)\right), \quad C_H = \left(\frac{H}{H_N}\right)^{3/2}, \quad n_t^r = \frac{n_t}{n_{tN}} \left(\frac{H}{H_N}\right)^{1/2} \tag{2}$$

where:

- n_t^r – relative water turbine velocity,
- C_H – water level coefficient,
- $a(\alpha)$, $b(\alpha)$, $c(\alpha)$ – function coefficients,
- α – guide vane angle [%].

The function coefficients were identified in the real hydropower plant with a propeller turbine. Taking the nominal parameters: Q_N, H_N, η_N, α_N, n_{tN} as reference values, the function coefficients can be approximated by the following functions [14].

$$\begin{aligned} a(\alpha) &= -0.44423\alpha^3 + 2.32343\alpha^2 - 3.12\alpha \\ b(\alpha) &= 3.6548\alpha^5 - 13.585\alpha^4 + 15.256\alpha^3 - 5.552\alpha^2 + 2.094\alpha \\ c(\alpha) &= -2.4484\alpha^5 + 10.09\alpha^4 - 13.493\alpha^3 + 5.872\alpha^2 + 0.347\alpha \end{aligned} \tag{3}$$

The shape of the turbine torque at different guide vane angles under constant water head is presented in Fig. 2.

The hydro-set model should include the dynamics of the water mass that is contained in the pipeline and the turbine. It is usually defined by the water inertia time constant (4) [15].

$$T_w = \frac{Q_N}{gH_N} \frac{L}{A} \tag{4}$$

where:

- g – gravity acceleration,
- L – pipeline length,
- A – cross section area of the pipeline.

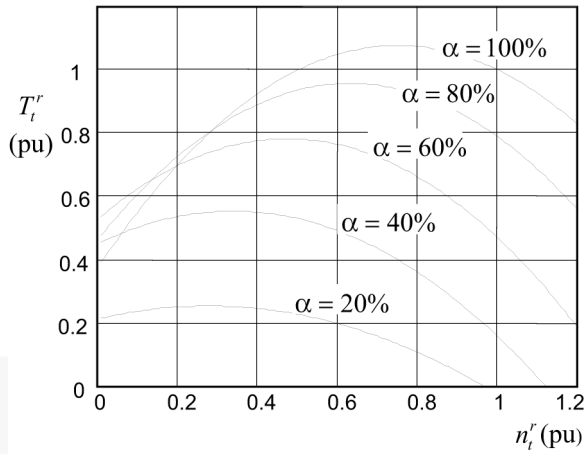

Fig. 2. Propeller turbine torque curves at different guide vane angles and nominal head in the per-unit system

The guide vane governor often operates based on the fluid drive system, where the movement is controlled by the electrically operated spool valve. The movement speed is determined by the fluid pressure and it is constant. Therefore, the model of the guide vane governor should include the speed limiter (R_s – raising and failing slew rate). The governor time constant is very small in comparison to the water inertia time constant, so it may be neglected.

The resulting hydro-set model containing the steady state relation of torque (2) with coefficients (3), water inertia time constant (4) and the governor speed limiter is presented in Fig. 3.

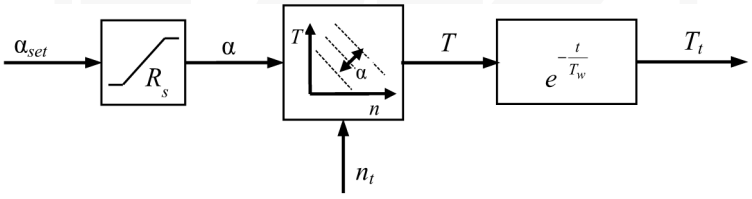

Fig. 3. Block diagram of the hydro-set model

4. SEIG model

The model of a three-phase squirrel-cage asynchronous machine is taken from the SimPowSys library. The model with a reference frame of rotor and Park transformation is used. The electrical part is represented by the four order state space model, while the mechanical part by the second order system [16]. The saturation of the mutual flux is specified by the curve of the stator voltage versus the stator current in the no-load state. The curve points are approximated by the piecewise linear relationship.

The capacitance value of the capacitor bank is assigned to the generator parameters in order to provide the excitation and may be obtained from the principle of *L-C* resonance according to the value (5).

$$C_g = \frac{1}{2\pi f\left(X_{\sigma s} + X_m\right)} \tag{5}$$

where:

f – voltage frequency,
$X_{\sigma s}$ – stator leakage reactance,
X_m – magnetizing reactance.

5. VC model

The VC is controlled using the space vector (SV) technique. The SV based modulation gives better voltage utilization and reduces the harmonics of output signals more than the conventional sinusoidal PWM technique [17]. The block diagram of the SV generator is presented in Fig. 4. The sector selector indicates one of the six sectors, depending on the actual voltage angle. Then, the duration time block calculates the time duration of two adjustment active vectors (T_i, T_j) for a given sector from the sector number, voltage angle, reference line voltage U_{ref}, actual DC voltage U_{dc} and switching period T_s. The modulation index m is defined by (6).

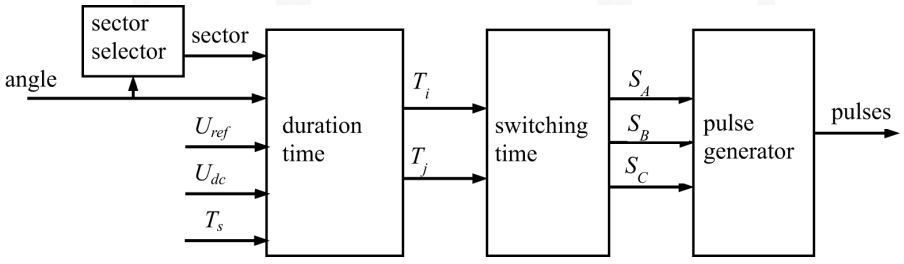

Fig. 4. Block diagram of the space vector generator.

$$m = \sqrt{3}\frac{U_{ref}}{U_{dc}} \quad \text{where: } 0 \le m \le \sqrt{2} \tag{6}$$

The timing sequence for each transistor (S_A, S_B, S_C) is estimated by the SVPWM switching patterns at each sector in the switching time block. Pulses for IGBT transistors are generated in the pulse generator block by comparing the switching timing signals with a triangle wave signal.

The presence of the capacitor bank decreases the VC reactive power necessary to regulate the voltage magnitude. It also constitutes with the VC inductance (reactor) the low pass filter. The inductance value L_{vc} can be calculated depending on the cut off frequency f_c (7). Furthermore, the minimum cost, losses and weight criteria should be taken into consideration [18].

$$L_{vc} = \frac{1}{\left(2\pi f_c\right)^2 C_g} \tag{7}$$

The battery model is characterized by the following parameters: nominal voltage U_{batt}, rated capacity Q_{batt} and the shape of the discharge characteristics. The discharge characteristics depend on the battery type. The battery used in the BEES is a Lithium-Ion battery because of the low internal resistance. The battery parameters have to be set mainly depending on the load value and guide vane governor. The maximal discharge current is determined by the load value for the minimal possible DC voltage, while the dynamics of the guide vane governor define the battery capacity and the discharge curve shape. The main condition is enough to keep the high DC voltage for the VSI to provide AC voltage higher than the nominal load voltage according to the formula: $U_{dc} > \sqrt{\frac{3}{2}} U_l$. The battery should maintain a DC voltage higher than 500 V under the maximal discharge current $I_{\text{batt}}^{\max}$ for the specific time. This time, defined by the hydro-set slew rate $T_{\text{batt}} \geq 1/R_s$, is enough to change the guide vane angle from 0 to 100% by the governor. The battery parameters are given in the Appendix and the battery discharge curve is presented in Fig. 5.

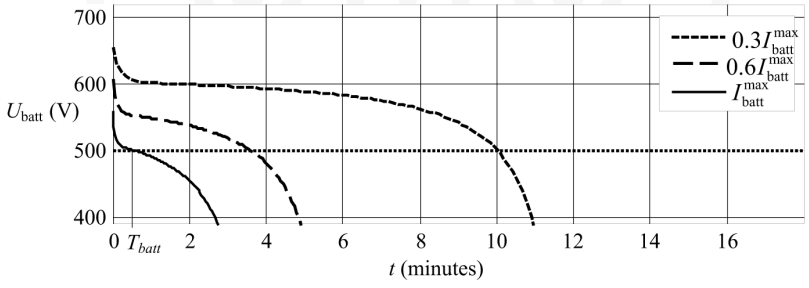

Fig. 5. Discharge curve of the Lithium-Ion battery (parameters given in the Appendix) under different discharge currents

6. Control strategy

The VC aim is to control the voltage of the load in magnitude and frequency. A simplified equivalent circuit of the VC connected to the load line through the impedance Z_{vc} is presented in Fig. 6.

The power flow at the connection point is described as follows [19].

$$\begin{aligned} \underline{S}_{vc} &= P_{vc} + jQ_{vc} = \underline{U}_l \overset{*}{\underline{I}} = \underline{U}_l \left(\frac{\underline{U}_l - \underline{U}_{vc}}{\underline{Z}_{vc}} \right)^* = U_g \left(\frac{U_l - U_{vc} e^{j\varphi_0}}{Z_{vc} e^{-j\vartheta}} \right) = \\ &= \frac{U_l^2}{Z_{vc}} e^{j\vartheta} - \frac{U_l U_{vc}}{Z_{vc}} e^{j(\vartheta+\varphi_0)} \end{aligned} \tag{8}$$

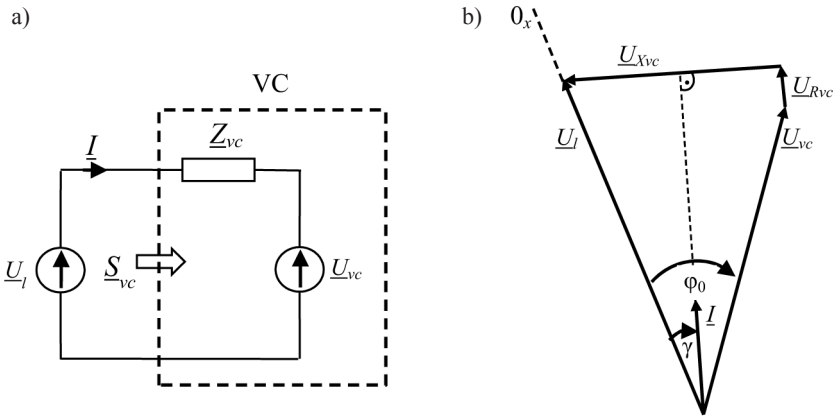

Fig. 6. VC connected to the load line: a) equivalent circuit, b) phasor diagram

The active and reactive power component can be calculated by separating the real and imagined part.

$$P_{vc} = \frac{U_l^2}{Z_{vc}}\cos(\vartheta) - \frac{U_l U_{vc}}{Z_{vc}}\cos(\vartheta + \varphi_0) \quad Q_{vc} = \frac{U_l^2}{Z_{vc}}\sin(\vartheta) - \frac{U_l U_{vc}}{Z_{vc}}\sin(\vartheta + \varphi_0) \tag{9}$$

Introducing $\vartheta = \text{arctg}\left(\frac{X_{vc}}{R_{vc}}\right)$, these formulas may be presented as:

$$P_{vc} = \frac{U_l}{Z_{vc}^2}\left[R_{vc}\left(U_l - U_{vc}\cos(\varphi_0)\right) + X_{vc}U_{vc}\sin(\varphi_0)\right]$$

$$Q_{vc} = \frac{U_l}{Z_{vc}^2}\left[-R_{vc}U_{vc}\sin(\varphi_0) + X_{vc}\left(U_l - U_{vc}\cos(\varphi_0)\right)\right] \tag{10}$$

Assuming that the inductance is dominant, $X_{vc} >> R_{vc}$ the resistance can be neglected. Moreover, considering the small value of the phase φ_0 ($\varphi_0 < 10°$), which results in $\sin(\varphi_0) \approx \varphi_0$ and $\cos(\varphi_0) \approx 1$, the equations (10) may be simplified.

$$P_{vc} = \frac{U_l U_{vc}}{X_{vc}}\varphi_0, \quad Q_{vc} = \frac{U_l}{X_{vc}}(U_l - U_{vc}) \tag{11}$$

The above formulas (11) mean that the active power depends mainly on the voltage phase φ_0 of the VC, while the reactive power depends on the voltage difference $U_l - U_{vc}$.

The frequency control is provided by the voltage phase of the VC. The voltage angle is set in the SVM generator and defined by the system frequency and the phase $\varphi = \omega_{vc}t + \varphi_0 = 2\pi f_{vc}t + \varphi_0$. In the situation when the active power of the load equals the generated power, the voltage phases of the load and the VC are equal, then $\varphi_0 = 0$ and $P_{vc} = 0$. Any disturbances of the system frequency (phase), caused by the surplus or deficiency of the active power in the system, is compensated by the active power provided

by the VSI. The surplus energy charges the battery, while the deficiency of active power discharges it.

The voltage magnitude of the SEIG depends on the reactive power value. The VC can provide additional reactive power in order to maintain the magnitude at the constant level. This is done with the value of the reference voltage, which is set in the SVM generator. The reference voltage is related to the modulation index (6) by the DC voltage, which value can vary according to the battery charge. The reference voltage is adjusted by the PI controller in the closed loop control based on the actual error (Fig 7). The PI error is calculated based on the RMS value of the line voltage. The line voltage can be estimated from the 3- instantaneous line voltages using formula (12) and it is filtered by the low pass filter (f_n – natural frequency, ζ – damping ratio).

$$U_{\mathrm{RMS}} = \sqrt{\frac{1}{3}\left(u_a^{\,2} + u_b^{\,2} + u_c^{\,2}\right)} \tag{12}$$

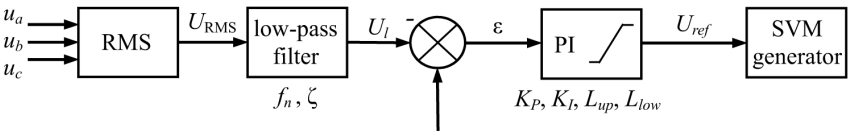

Fig. 7. Controller of the voltage magnitude (reactive power controller)

The state of the battery charge has to be controlled in order to provide the minimum DC voltage value necessary to obtain the fundamental line-voltage amplitude at about 400 V. This is the task of the guide vane controller (Fig. 8). The fully charged battery voltage is the set point. The PI regulator adjusts the set angle of the guide vanes, which is the input of the hydro-set model (Fig. 3). The Hydro-set model calculates the actual turbine torque that is transferred by the gearbox of the gear ratio R_g which matches the generator and turbine speeds.

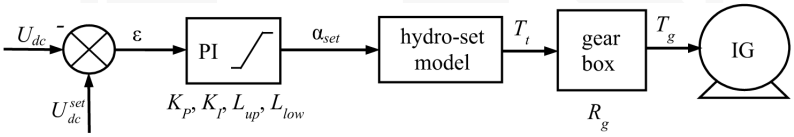

Fig. 8. Guide vane controller (battery charge controller)

7. Simulation results

The simulations have been performed in the Matlab/Simulink software with parameters and rated data given in the Appendix. The ready elements: induction motor, battery, universal bridge are taken from the SimPowerSys toolbox. The prepared model is solved in a discrete mode with $1 \cdot 10^{-6}$ s of sample time using the Tustin method. The initial conditions concern the generator slip (0.01) and the capacitor bank voltages (50 V, –25 V, –25 V).

The simulation presents time domain signals of the system disturbed by the changing load. The step changes of the load that affects the magnitude and frequency of the load voltage have been analyzed. The simulation sequence is as follows.

At the beginning the voltage build-up process with no load, that takes about 1 s, is visible (Fig. 9). After 4 seconds when the line voltage equals 400 V the three-phase load (P_l = 3.5 kW, Q_l^{ind} =1 kVar) is connected. A small dip of the voltage and frequency at this time is visible; however, the voltage controller reaches the set point within 1s after the disturbance. In order to keep the frequency constant, the VC supplements the active power of the load, while the guide vane governor is adjusting (Fig. 10). Initially, it covers all of the load power demand. This process takes time due to the long hydro-set time constants. In the steady state, the total active power of the load is provided by the induction generator.

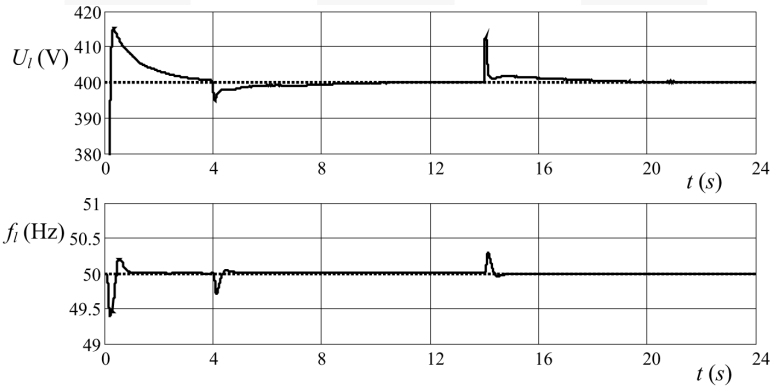

Fig. 9. Variations of the voltage in magnitude and frequency of the load

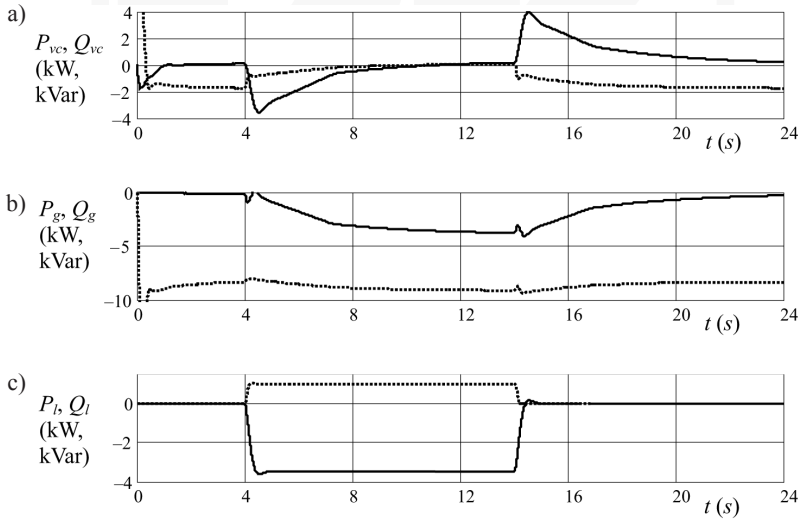

Fig. 10. Active (solid line) and reactive (dotted line) power flow: a) VC, b) generator, c) load

At t = 14 s the load is switched off what causes the voltage and frequency increase. These perturbations are quickly eliminated by the VC which absorbs the surplus power in the battery. The battery current (Fig. 11) which corresponds to the charging process indicates the battery contribution in the control process for about 8 seconds after the load disturbance. At this time the battery energy is compensated to its nominal capacity by the guide vane controller which monitors the battery voltage.

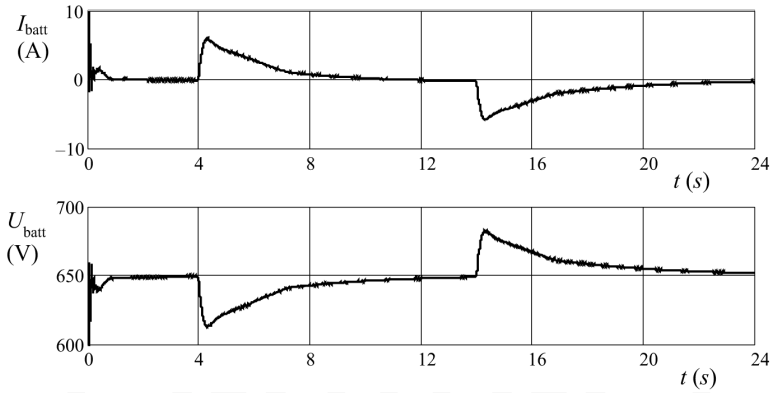

Fig. 11. Current and voltage of the battery

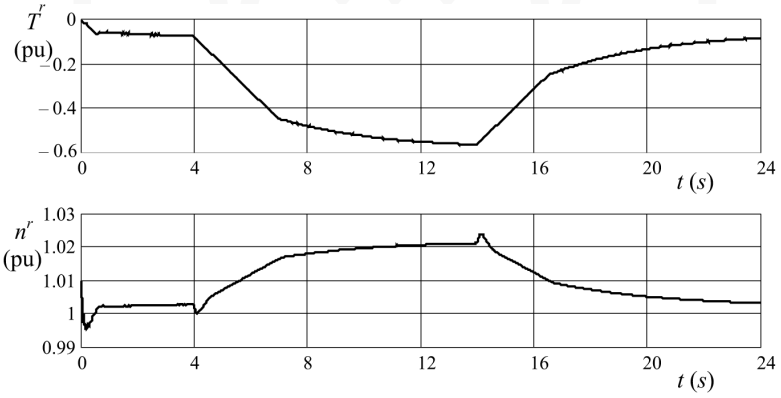

Fig. 12. Relative values of torque and speed of the generator

The turbine governor adjusts the generator's torque through the guide vane angle according to the battery voltage (Fig. 12). This affects the generator speed, which is additionally disturbed by the load variations.

The aim of the control system in the form of the voltage in magnitude and frequency stabilization is achieved with the satisfactory static and dynamic results. The SEIG in cooperation with the VC provide the active and reactive energy, according to the load demand (Fig. 10c).

8. Conclusions

The presented test shows the system dynamic performance under step changes of the electrical load. The voltage and frequency variations are minimized by using the VC, which acts as a controllable active and reactive power source. The energy buffer (battery) provides the active power necessary to maintain a constant frequency. The presented system uses the guide vane governor that controls the DC voltage of the battery. This solution minimizes the size of the battery of which energy is utilized only for a short time after the load disturbance when the guide vane governor is adjusting. Moreover, the VC decreases the negative dynamic stress of the hydro-set during the load disturbance. The presented frequency stabilization with variations of less than 0.5 Hz is not achievable by conventional speed governors due to the large turbine time constants. The VC can also compensate the reactive power of the load. By adding the VC to the conventional small reservoir hydropower plant with an induction generator and a guide vane governor, it is possible to achieve an autonomous generating system, which provides voltage and frequency stabilization.

Acknowledgment

The presented results of the research, which was carried out under the theme No. E-2/580/2016/DS, were funded by the subsidies on science granted by Polish Ministry of Science and Higher Education.

Appedndix

Hydro-set model	SEIG model	VC model	Voltage controller	Guide vane controller
$Q_N = 1\ m^3/s$ $H_N = 1\ m$ $\eta_N = 0.75$ $\alpha_N = 100\%$ $n_{tN} = 600\ rpm$ $g = 9.81\ m/s^2$ $L = 5\ m$ $A = 0.24\ m^2$ $T_w = 2.12\ s$ $R_s = 20\%/s$	$P_N = 7.5\ kW$ $U_N = 400\ V$ $n_N = 1440\ rpm$ $X_{\sigma s} = 0.226\ \Omega$ $X_m = 13.04\ \Omega$ $C_g = 480\ \mu F$ $R_g = 2.6$	$T_s = 0.0002\ s$ $L_{vc} = 1\ mH$ $U_{batt} = 600\ V$ $U_{batt} = 1\ Ah$ $I_{batt}^{max} = 15\ A$ $T_{batt} = 25\ s$ $\omega_{vc} = 100\ \pi\ rad/s$ $C_{dc} = 2\ mF$ $f_c = 112\ Hz$	$f_n = 20\ Hz$ $\zeta = 1$ $U_l^{set} = 400\ V$ $K_P = 1$ $K_I = 8$ $L_{up} = 420\ V$ $L_{low} = 370\ V$	$U_{dc}^{set} = 650\ V$ $K_P = 0.003$ $K_I = 0.02$ $L_{up} = 1.1$ $L_{low} = 0$

References

[1] Singh G.K., *Self-excited induction generator research – a survey*, Electric Power Systems Research, vol. 69, 2004, 107–114.

[2] Bansal R., *Three-phase self-excited induction generators an overview*, IEEE Transactions on Energy Conversion, vol. 20(2), 2005, 292–299.

[3] Alnasir Z., Kazerani M., *Performance comparison of standalone SCIG and PMSG-based wind energy conversion systems*, IEEE 27th Canadian Conference on Electrical and Computer Engineering (CCECE), Toronto, 4–7 May 2014, 1–8.

[4] Haque M.H., *Voltage regulation of a stand-alone induction generator using thyristor-switched capacitors*, IEEE International Conference on Sustainable Energy Technologies, Singapore, 24–27 Nov. 2008, 34–39.
[5] Ahmed T., Noro O., Nakaoka M., *Terminal voltage regulation characteristics by static var compensator for a three-phase self-excited induction generator*, IEEE Transactions on Industry Applications, vol. 40(4), 2004, 978–988.
[6] Suarez E., Bortolotto G., *Voltage-frequency control of a self excited induction generator*, IEEE Trans. on Energy Convers., vol. 14(3), 1999, 394–401.
[7] Marra E., Pomilio J., *Self-excited induction generator controlled by a VS-PWM bidirectional converter for rural applications*, IEEE Transactions on Industry Applications, vol. 35(4), 1999, 877–883.
[8] Marra E.G., Pomilio J.A., *Induction-generator-based system providing regulated voltage with constant frequency*, IEEE Transactions on Industrial Electronics, vol. 47(4), 2000, 908–914.
[9] Chilipi R.R., Singh B., Murthy S., *A new voltage and frequency controller for standalone parallel operated self excited induction generators*, Int. J. Emerg. Elect. Power Syst., vol. 13(1), 2012, 1–17.
[10] Chilipi R.R., Singh B., Murthy S.S., *Performance of a Self-Excited Induction Generator With DSTATCOM-DTC Drive-Based Voltage and Frequency Controller*, IEEE Transactions on Energy Conversion, vol. 29(3), 2014, 545–557.
[11] Jakubowski B., Pieńkowski K., *Analysis and synthesis of converter control system of autonomous induction generator with field oriented control*, Archives of Electrical Engineering, vol. 62(2), 2013, 267–279.
[12] Singh B., Kasal G.K., *Voltage and Frequency Controller for a Three-phase Four-wire Autonomous Wind Energy Conversion System*, IEEE Transaction on Energy Conversion, vol. 23(2), 2008, 509–518.
[13] Barrado J., Grino R., Valderrama-Blavi H., *Power-quality improvement of a stand-alone induction generator using a statcom with battery energy storage system*, IEEE Trans. Power Del., vol. 25(4), 2010, 2734–2741.
[14] Borkowski D., *Performance analysis of the Single-Phase Grid-Connected Inverter of a photovoltaic system in water and wind applications*, E3S Web of Conferences, SEED, vol. 10, 2016, no. 00004.
[15] Zoby M.R.G., Yanagihara J.I., *Analysis of the primary control system of a hydropower plant in isolated model*, Journal of the Brazilian Society of Mechanical Sciences and Engineering, vol. 31, 2009, 5–11.
[16] Boldea I., *The Electric Generators Handbook, Volume II: Variable speed generators*. CRS Press, Boca Raton USA 2006.
[17] Mohan N., Undeland T.M., Robbins W.P., *Power Electronics: Converters, Applications and Design*, Wiley, New York 1996.
[18] IEEE Standard 519-1992: IEEE Recommended Practices and Requirements for Harmonic Control in Electrical Power Systems, New York, USA, 1993.
[19] De Brabandere K., Bolsens B., Van den Keybus J., Woyte A., Driesen J. and Belmans R., *A Voltage and Frequency Droop Control Method for Parallel Inverters*, IEEE Transactions on Power Electronics, vol. 22(4), 2007, 1107–1115.